Supporting information

Hydrofunctionalization of olefins to value-added chemicals via photocatalytic coupling

Yonghui Fan,[a,b] Shenggang Li,[a,c] Jingxian Bao,[a,b] Lei Shi,[a,b] Yanzhang Yang,[a,d] Fei Yu,[a,d] Peng Gao,[a] Hui Wang,[a] Liangshu Zhong,*[,a,c] and Yuhan Sun*[,a,c]

[a] Key Laboratory of Low-Carbon Conversion Science and Engineering, Shanghai Advanced Research Institute, Chinese Academy of Sciences, Shanghai 201203, China

[b] Department of Chemistry, College of Sciences, Shanghai University, Shanghai 200444, China

[c] School of physical Science and Technology, ShanghaiTech University, Shanghai 201210, China

[d] University of the Chinese Academy of Sciences, Beijing 100049, China

* E-mail: zhongls@sari.ac.cn; sunyh@sari.ac.cn

Contents

1. Experiment methods

1.1. Chemicals

The TiO_2 (P25) nanoparticles were purchased from ACROS ORDANIC. $H_2PtCl_6 \cdot 6H_2O$ (99%), $HAuCl_4 \cdot 3H_2O$ (99.9%), $RuCl_3 \cdot xH_2O$ (35.0-42.0%), $PdCl_2$ (59-60%), methanol (99.5%), acetone (99.5%), acetonitrile (99%) and ethyl acetate (99.5%) were purchased from Sinopharm Chemical Reagent Co. LTD. Dodecane (99.5%), 1-decene (95%), 1-nonene (90%), 1-octene (99.5%), 1-heptene (99.5%), 1-hexene (99.5%), 1,9-decadiene (98%), 4-phenyl-1-butene (98%) and 10-undecene-1-ol (99%) were purchased from Shanghai Aladdin Biochemical Technology Co .LTD. Deionized water (18.25 $M\Omega \cdot cm^{-1}$) supplied by an UP Water Purification System was used in the experimental processes.

1.2. Photocatalyst preparation

The catalysts including Pt/TiO_2, Pd/TiO_2, Ru/TiO_2 and Au/TiO_2 were prepared by impregnation method. The commercial P25 (5 g) was dispersed in the deionized water (25 mL). 6 mL H_2PtCl_6 solution (0.01 g/mL for Pt), 10 ml $PdCl_2$ solution (0.007 g/mL for Pd), 12 ml $RuCl_2$ solution (0.008 g/mL for Ru) or 5 mL $HAuCl_4$ solution (0.01 g/mL for Au) was added to this slurry. The mixture was stirred for 1 h at room temperature and dried at 60 °C with vacuum drying oven for overnight. The catalyst was reduced in H_2 with a gas-flow rate of 100 mL/min and at 300 °C for 180 min with the heating ramp of 1 °C min^{-1}. The temperature was dropped to room temperature in Ar (99.99%) flow, and then the catalyst was passivated for 1 h in 1% O_2/Ar (v/v) with a gas-flow rate of 10 ml/min for further usage.

1.3. Photocatalyst characterization

Transmission electron microscopy (TEM), high-resolution transmission electron microscopy (HRTEM) were performed on a JEM-2100F microscope at an acceleration voltage of 200 kV. The XRD patterns were performed on a Rigaku Ultima IV X-ray powder diffractometer using Cu Kα radiation with a wavelength of 1.54056 Å at 40 kV and 40 mA. The UV-Vis spectra (DRS) were recorded on a Shimadzu DUV-3700 spectrophotometer. X-ray photoelectron spectra (XPS) were acquired on an ESCALAB MKII with Mg Kα (hυ = 1253.6 eV) as the excitation source. Inductively Coupled Plasma

(ICP) analysis of platinum, gold, palladium and ruthenium was performed using an ICP optical emission spectrometer (Perkin Elmer).

1.4. Radical trapping study

The EPR studies were carried out in a quartz tube, and the spectra recorded on a Bruker EPR ELEXSYS 500 spectrometer equipped with an in situ irradiation source (a Quanta-Ray Nd: YAG laser system with λ = 355 nm). Methanol or methanol-H_2O solution containing 0.1 M 5,5-dimethyl-1-pyrroline-N-oxide (DMPO) and 1 mg/ml Pt/TiO_2 were used for EPR experiments. All samples were made in glovebox. During the EPR photochemical experiments, the samples were irradiated at 25 °C directly in the EPR resonator, and the EPR spectra were recorded in situ during a continuous photoexcitation. The operating condition was as follows: microwave frequency ν = 9.51 GHz, power of microwave W = 10.1 mW, scanning range 3330–3430 G. The g-values (2.0081±0.0001) were determined using a built-in magnetometer. The EPR spectra obtained were analyzed and simulated using the winsim software.

1.5. Photocatalytic evaluation

Photocatalytic reactions were carried out in a 100 mL sealed micro stainless autoclave with 40 mm diameter sapphire window. Typically, 50 mg of solid photocatalyst was suspended in the solution containing 50 mL methanol and 2 mL deionized water. 1-Decene (1 mmol) and dodecane (as the internal standard) were added to the above mixture. The reactor was filled with Ar to avoid the existence of O_2. Typically, the light source was a 300 W Xe lamp (CEL-HXUV300, Beijing Aulight) with ultraviolet (UV) light source (200-400 nm) with intensity of 100 mW/cm^2. The photocatalytic reaction was performed at 60℃ for 15 h. After the reaction, the sample was analyzed by GC-MS (Agilent 7890A) with MS detector. The Product quantification was calculated according to an internal standard method. Photocatalytic performance with time-on-stream was carried out in a 200 mL quartz autoclave with 40 mm diameter window with a rubber plug at the reactor side. After illumination, the sample was collected at different reaction time.

Turnover number (TON) based on the target product was calculated according to:

TON × 10^3 = (moles of target product) / (moles of photocatalyst) × 10^3

Turnover frequency (TOF) based on the target product was calculated according to:

TOF (h^{-1}) × 10^3 = Turnover number / Reaction time × 10^3

Selectivity to the target product was calculated according to:

Selectivity (%) = (moles of target product) / (moles of all products)

Anti-Markovnikov regioselectivity was calculated according to:

Anti-Markovnikov regioselectivity (%) = (moles of target product with anti-Markovnikov regioselectivity) / (moles of products with both anti-Markovnikov and Markovnikov regioselectivity)

The A/(A+ P) ratio was obtained according to:

A/(A+P) = (moles of alcohol product) / (moles of alcohol product + moles of paraffin product).

Three repeat experiments were carried out under the same reaction conditions and the relative error was typically within 5%.

1.6. Density Functional Theory Calculations

Molecular DFT calculations were performed to study the formation and reactions of the carbon-centred radical intermediates. The Gaussian 09 program[1] was used with the B3LYP exchange-correlation functional[2] and the DFT-optimized DZVP2 basis set[3]. Molecular models were visualized by the AGUI graphical interface from the AMPAC program [4].

2. Structure characterization of various photocatalysts

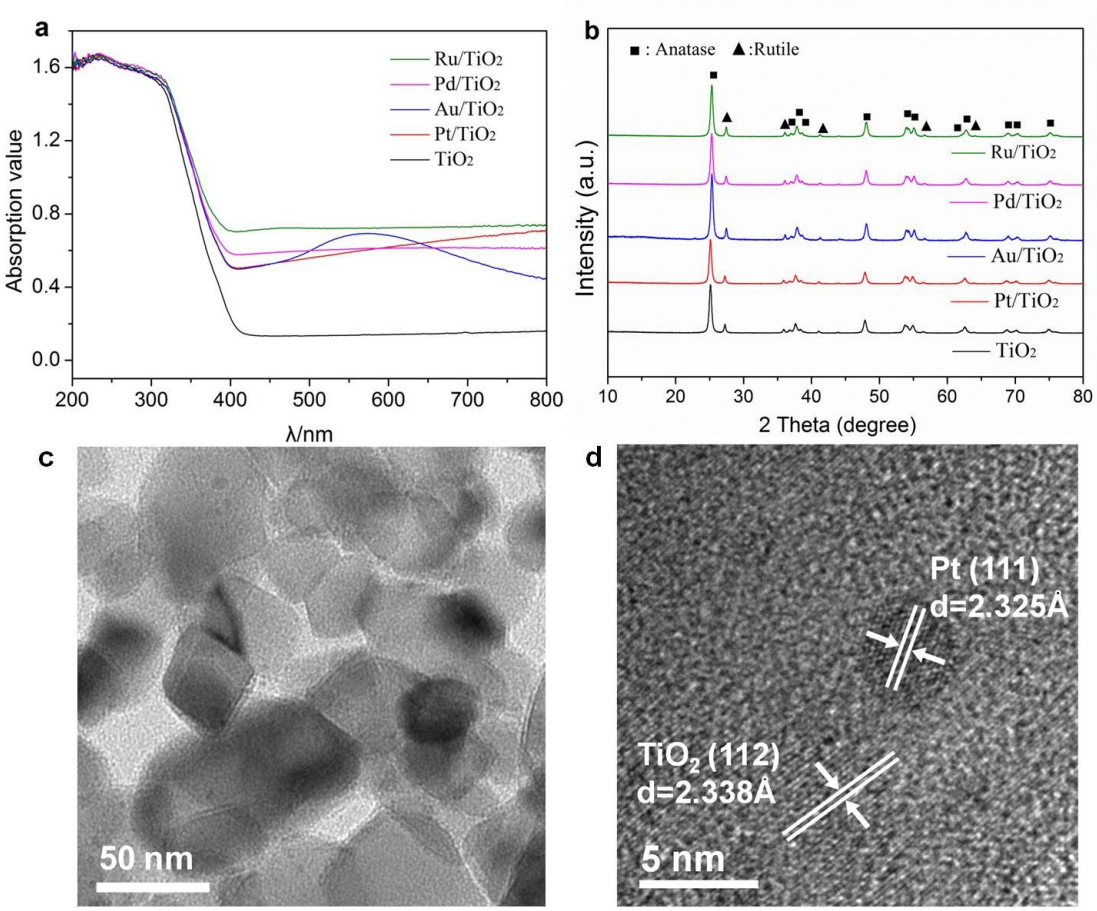

Figure S1. Structure characterization of various photocatalysts. **a**, UV−Vis spectra of various photocatalysts. The UV−Vis spectra indicated the adding of novel metals to TiO_2 could lead to slight red shift. Au/TiO_2 exhibited a definite absorption in the range from 500-600 nm due to surface plasma resonance (SPR) effect. **b**, XRD diffraction pattern. The XRD pattern revealed the diffraction peaks of both the anatase and rutile phases of TiO_2. No diffraction peaks of the noble metal particles were observed due to the low loading content. **c**, TEM image of Pt/TiO_2. **d**, High-resolution TEM image of Pt/TiO_2. Pt nanoparticles with the size of ~4 nm were observed.

3. Products analysis by GC-MS and reaction path for acetal

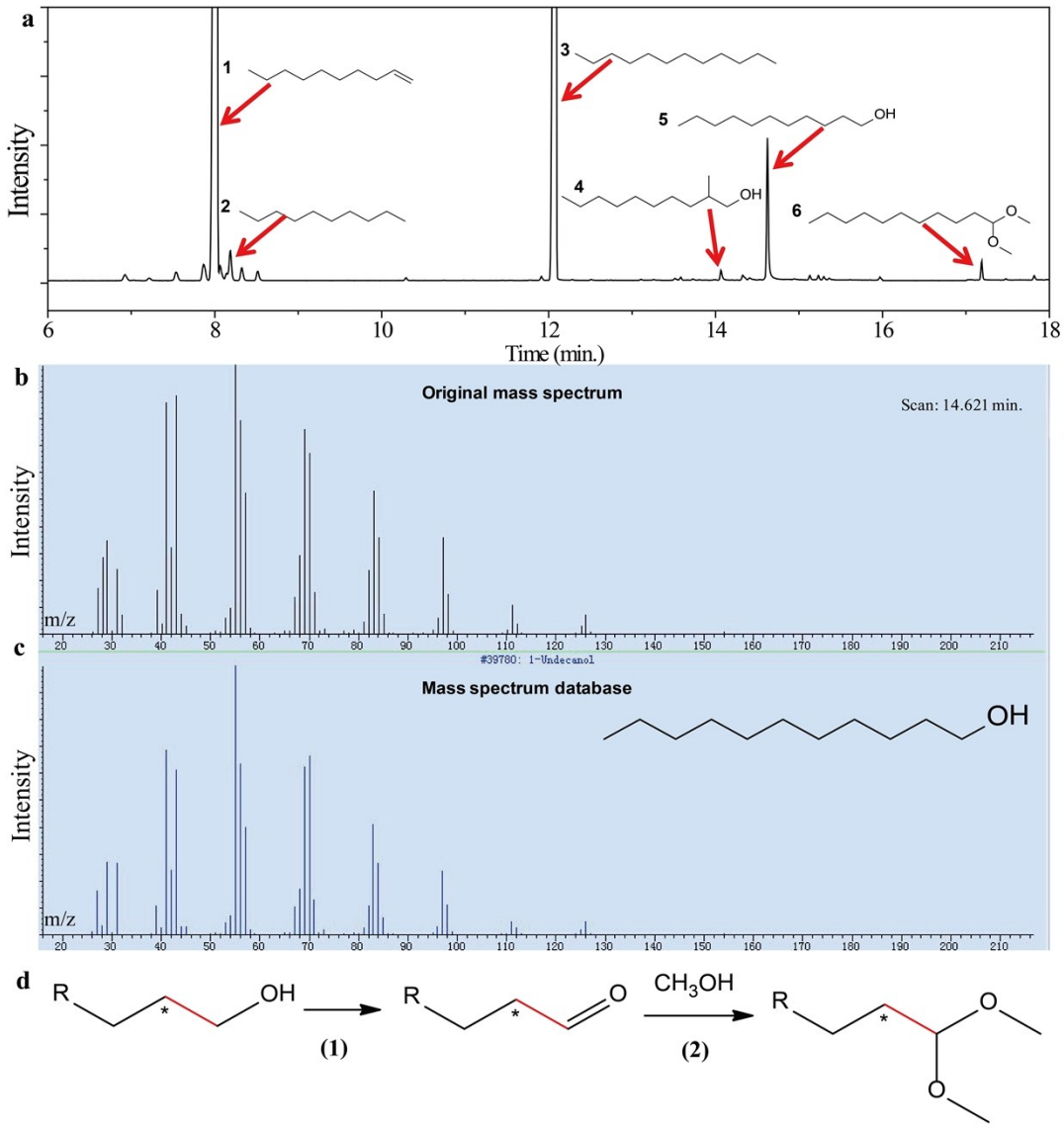

Figure S2. Products analysis by GC-MS and reaction path for acetal. **a**, GC-MS spectra for the products via photocatalytic coupling of 1-decene and methanol. 1:1-decene; 2: decane (byproduct); 3: dodecane (internal standard); 4: 2-methyl-1-decanol (Markovnikov product); 5: 1-undecanol (target product); 6: acetal compound (byproduct); other small peaks were impurities from feedstock. **b**, Original mass spectrum at 14.621 min for 1-undecanol product. **c**, Standard mass spectrum of 1-undecanol from the database. **d**, The reaction path for acetal as the main byproduct. Higher aliphatic alcohol was further oxidized by h^+ to aldehyde, which was then converted to acetal. The mass spectrum of other products were in Appendix diagram.

4. Effect of the reaction temperature on the catalytic performance

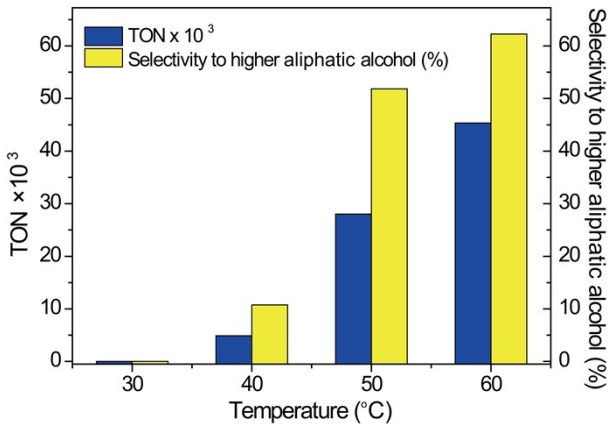

Figure S3. Effect of reaction temperature on the catalytic performance. Reaction condition: 1 mmol of 1-Decene，50 mg of photocatalyst in 50 mL of methanol. The reaction were respectively conducted under argon atomsphere at 30 °C, 40 °C, 50 °C, 60 °C under Xe lamp irradition (200-400 nm) with light intensity of 100 mW/cm^2. The reaction time was 15 h. TON and TOF were calculated based on the target product.

5. Effect of the adding amount of water on the catalytic performance

Table S1. Effect of the adding amount of water on the catalytic performance for hydrofunctionalization of 1-decene with methanol. The addition of appropriate amount of water into the reaction system ($V_{methanol}/V_{water}$ = 50/2 – 50/5) enhanced the catalytic activity and alcohol selectivity while excess water would weaken the photocatalytic performance ($V_{methanol}/V_{water}$ = 50/10).

$V_{methanol}/V_{water}$	TON $\times 10^3$	TOF(h^{-1}) $\times 10^3$	Selectivity to higher aliphatic alcohol (%)	A/(P+A)	Anti-Markovnikov regioselectivity (%)
50 : 0	29.6	2.0	50.4	0.61	93
50 : 2	45.3	3.0	62.3	0.92	93
50 : 5	103.2	6.9	50.6	0.85	92
50 : 10	56.5	3.8	19.5	0.63	92

6. The area ratio of XPS peaks

Table S2. The area ratio of XPS peaks. XPS O1s spectra for the sample can be de-convoluted into three distinct peaks: the main oxide peak at 530.3 eV ('$O_{lattice}$') and two additional peaks at 531.2 eV and 532.5 eV, which were assigned to O atoms next to a defect ('O_{defect}') and surface hydroxyls ('OH'), respectively. After reaction, the peaks area ratio of $O_{defect}/O_{lattice}$ increased to 0.67 from 0.26. Ti $2p_{3/2}$ spectra for the sample can be de-convoluted into two distinct peaks: the Ti^{4+} peak at 459.0 eV and Ti^{3+} peak at 457.9 eV, respectively. After reaction, the peaks area ratio of Ti^{3+}/Ti^{4+} increased to 0.21 from 0.10.

Peaks	O 1s			Ti $2p_{2/3}$	
	$O_{lattice}$	O_{defect}	OH	Ti^{3+}	Ti^{4+}
Binding energy (eV)	530.3	531.2	532.5	457.9	459.0
Pt/TiO_2 precursor	1	0.13	0.06	0.09	1
Fresh Pt/TiO_2	1	0.26	0.04	0.1	1
Spent Pt/TiO_2	1	0.67	0.25	0.21	1

7. *In situ* electron paramagnetic resonance (EPR) study

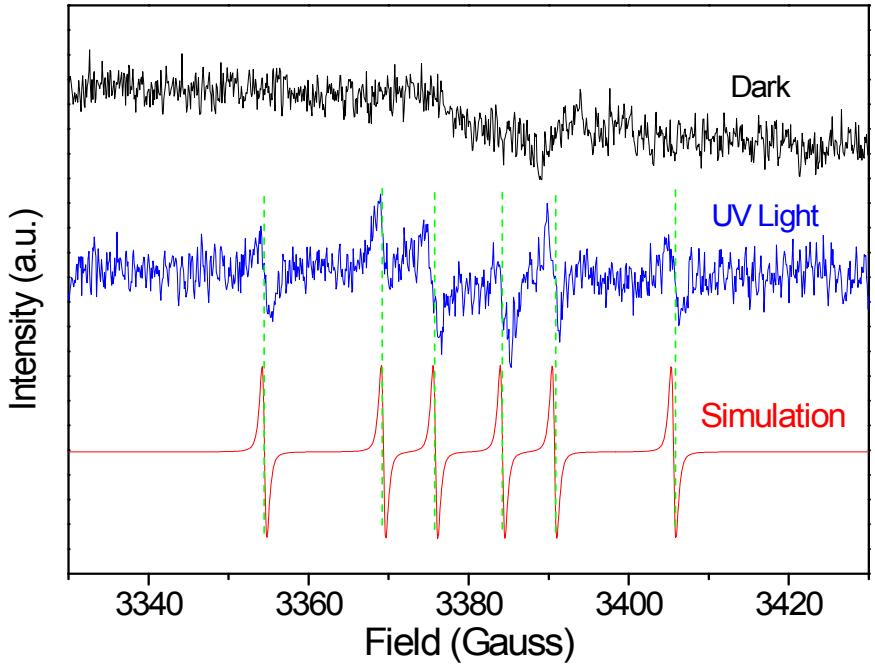

Figure S4. *In situ* electron paramagnetic resonance (EPR) study. EPR spectra in dark (black), irradiation by 355 nm light (blue) and the corresponding simulation data (red). EPR spectrum, which can be fitted into two hyperfine splitting constants, i.e., a_N = 14.9 G and a_H =21.3 G, was observed in the presence of Pt/TiO_2 under irradiation. The EPR spectrum could be ascribed to the DMPO-CH_2OH spin adduct, in which the interaction of the hydroxymethyl radical (·CH_2OH) with neighbouring nitrogen (I_N = 1) and hydrogen (I_H = 1/2) nuclei resulted in two hyperfine splitting constants.

8. Proposed mechanism for photocatalytic hydrofunctionalization of olefins

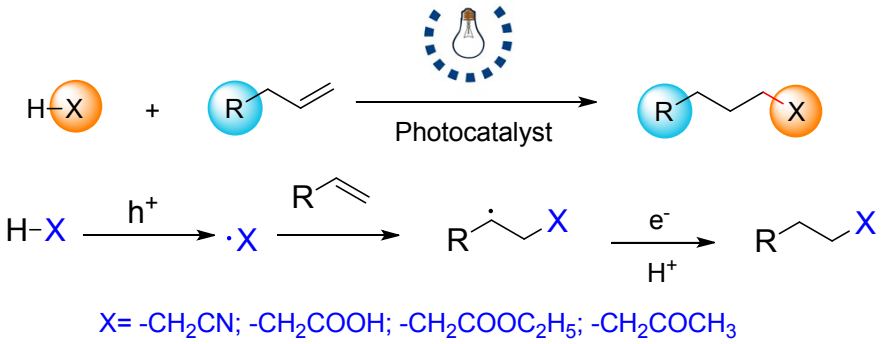

Scheme S1. Proposed mechanism for photocatalytic hydrofunctionalization of olefins.

Appendix diagram

(1): The mass spectrum of undecan-1-ol.

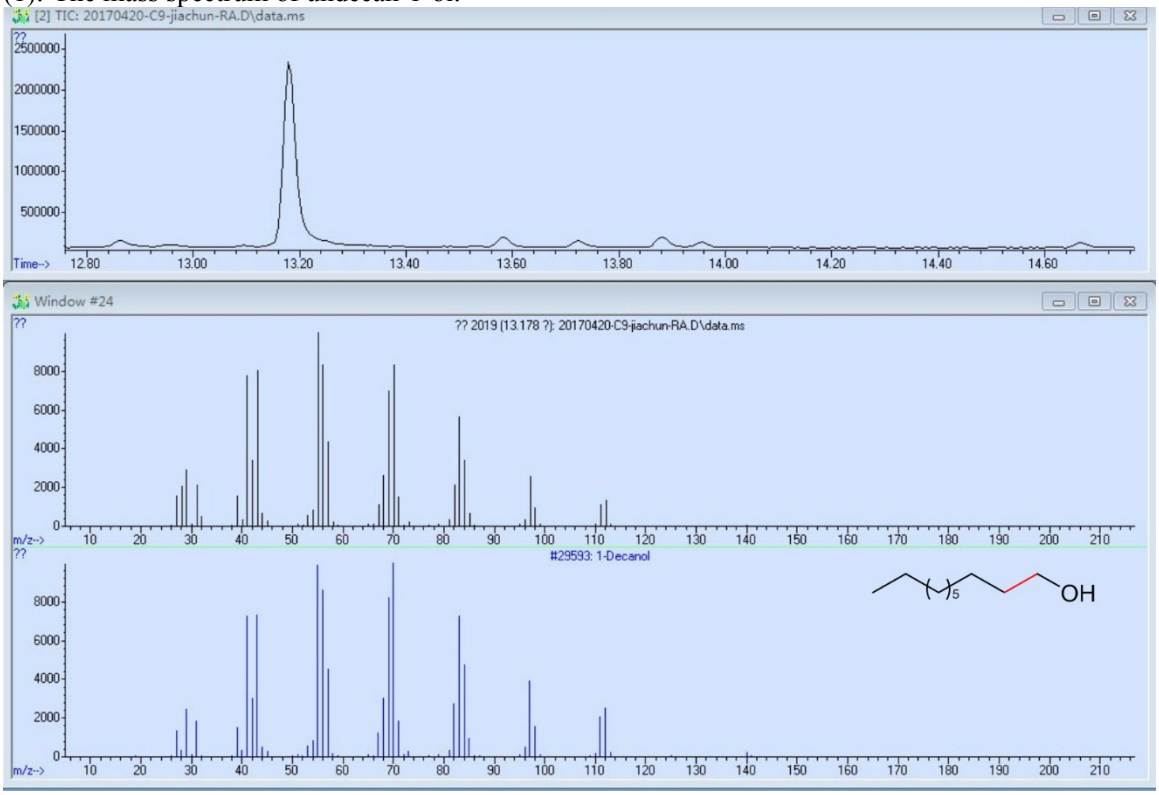

(2): The mass spectrum of decan-1-ol.

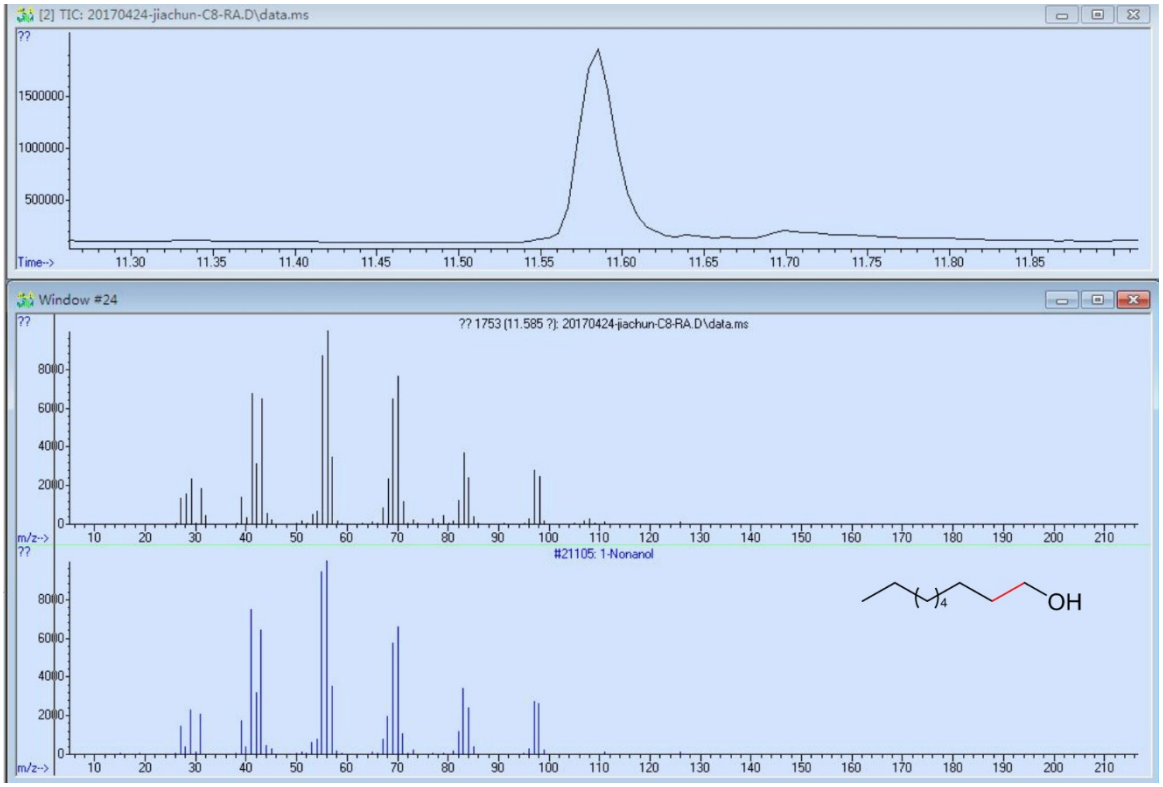

(3): The mass spectrum of decan-1-ol.

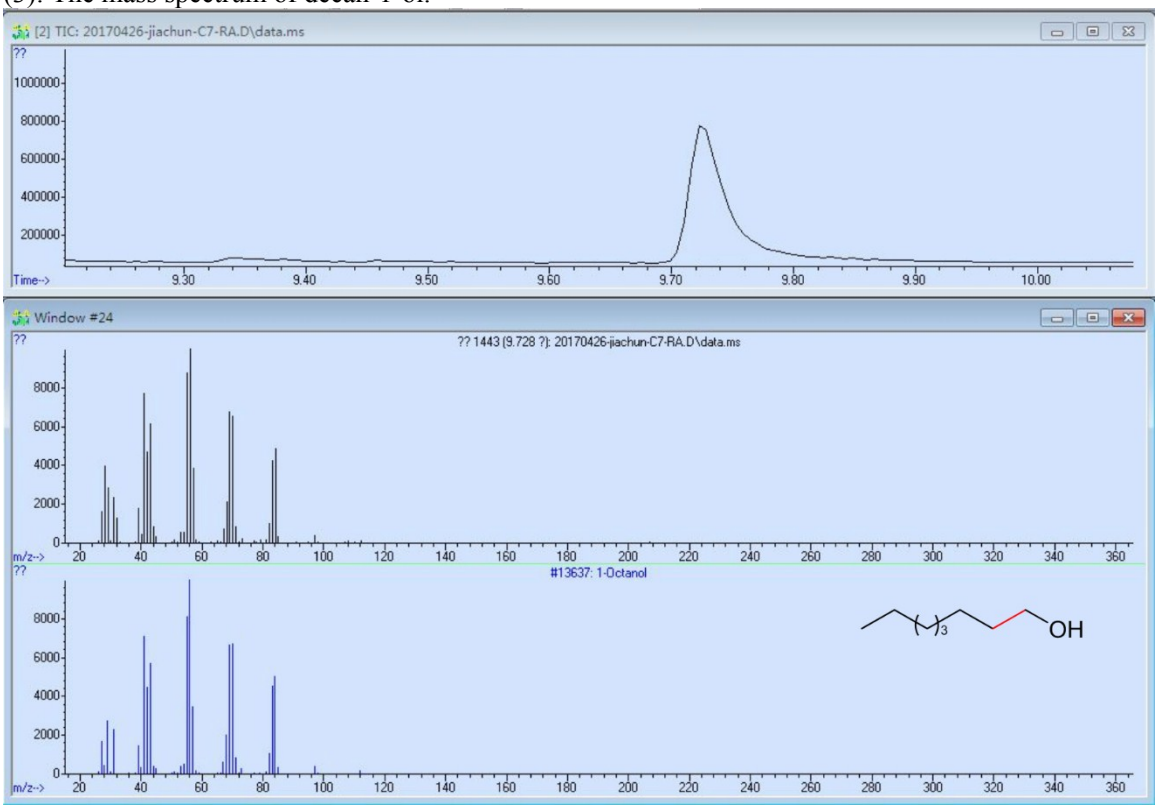

(4): The mass spectrum of dec-9-en-1-ol.

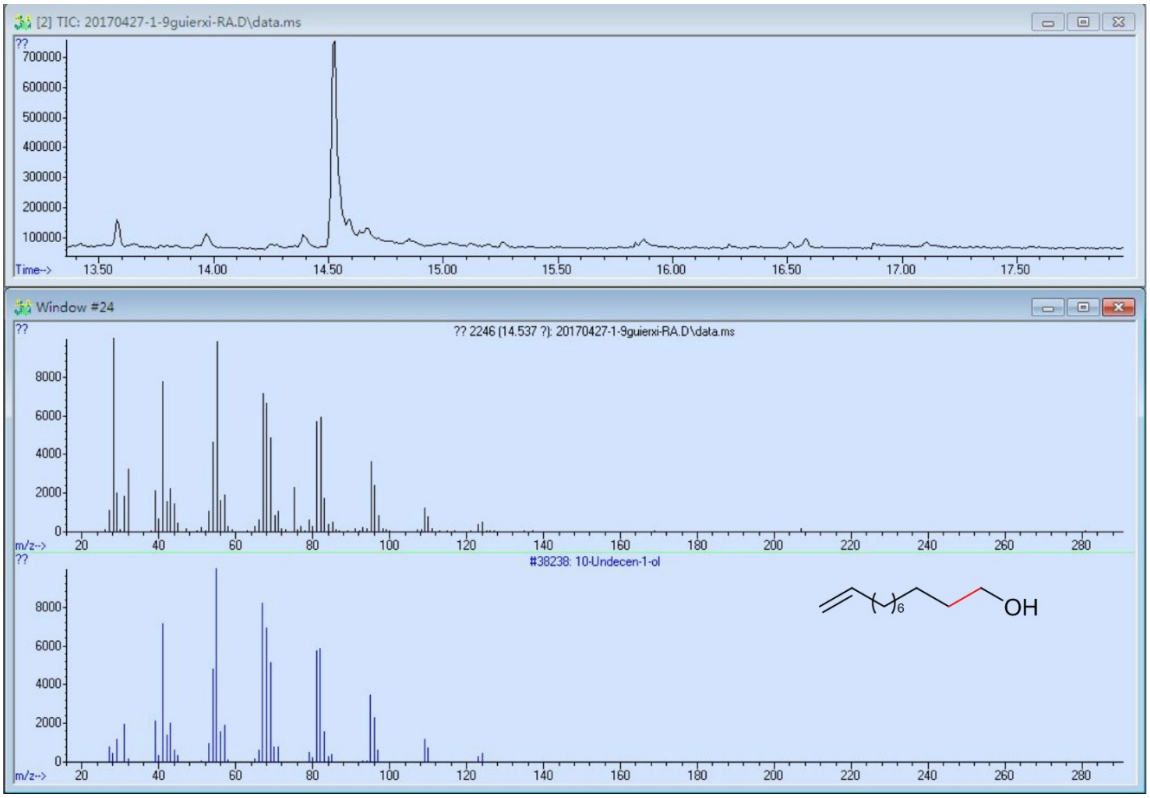

(5): The mass spectrum of tridecane-1,13-diol.

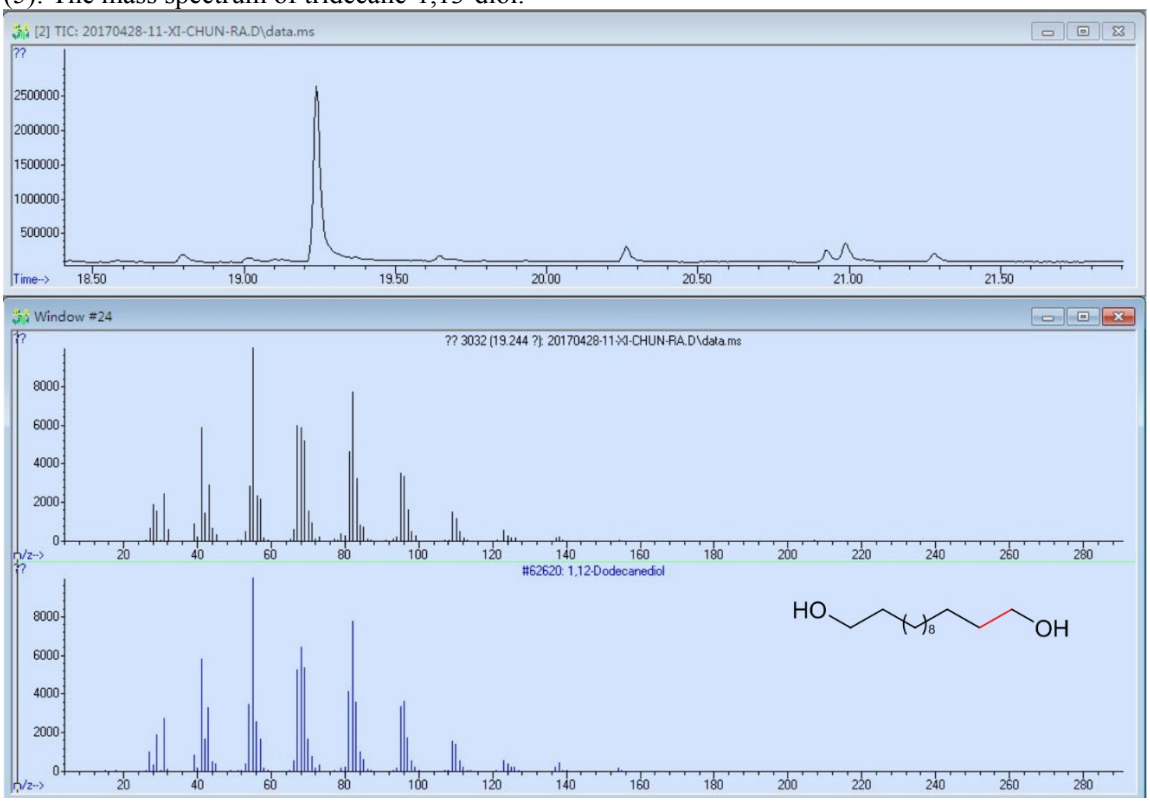

(6): The mass spectrum of 5-phenylpentan-1-ol.

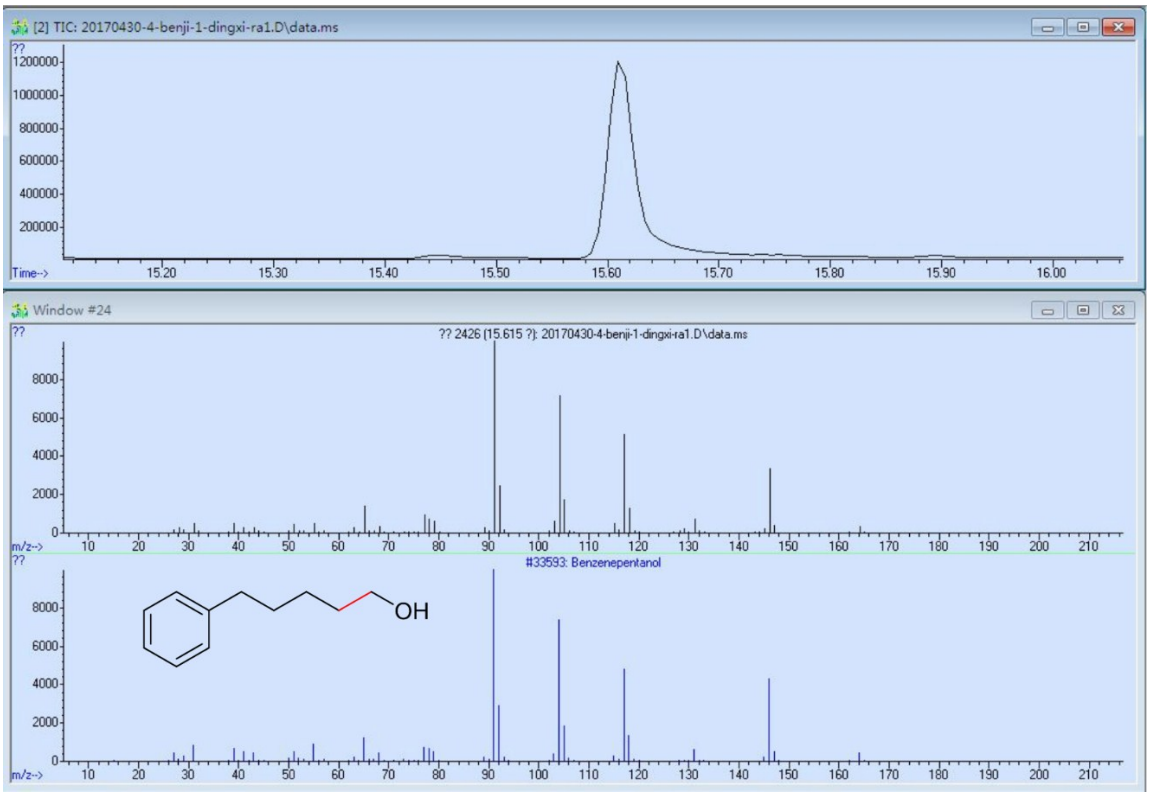

(7): The mass spectrum of dodecanenitrile.

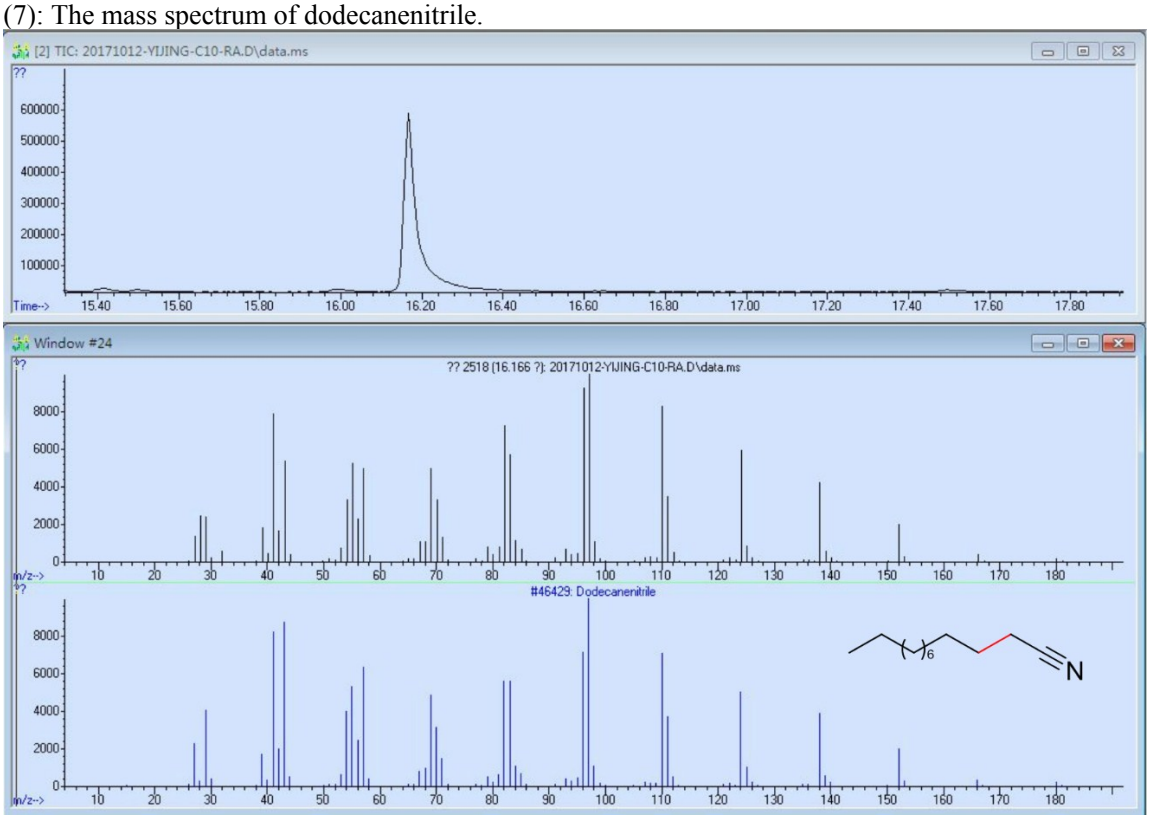

(8): The mass spectrum of undecanenitrile.

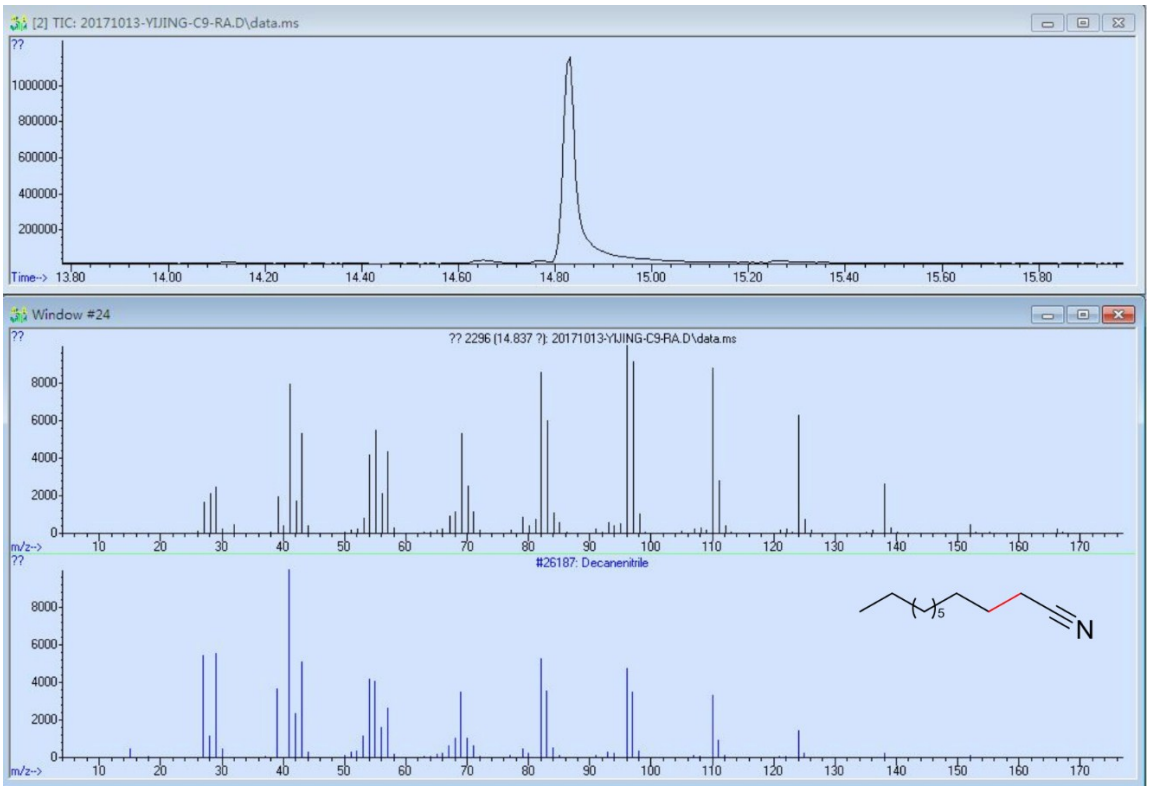

(9): The mass spectrum of decanenitrile.

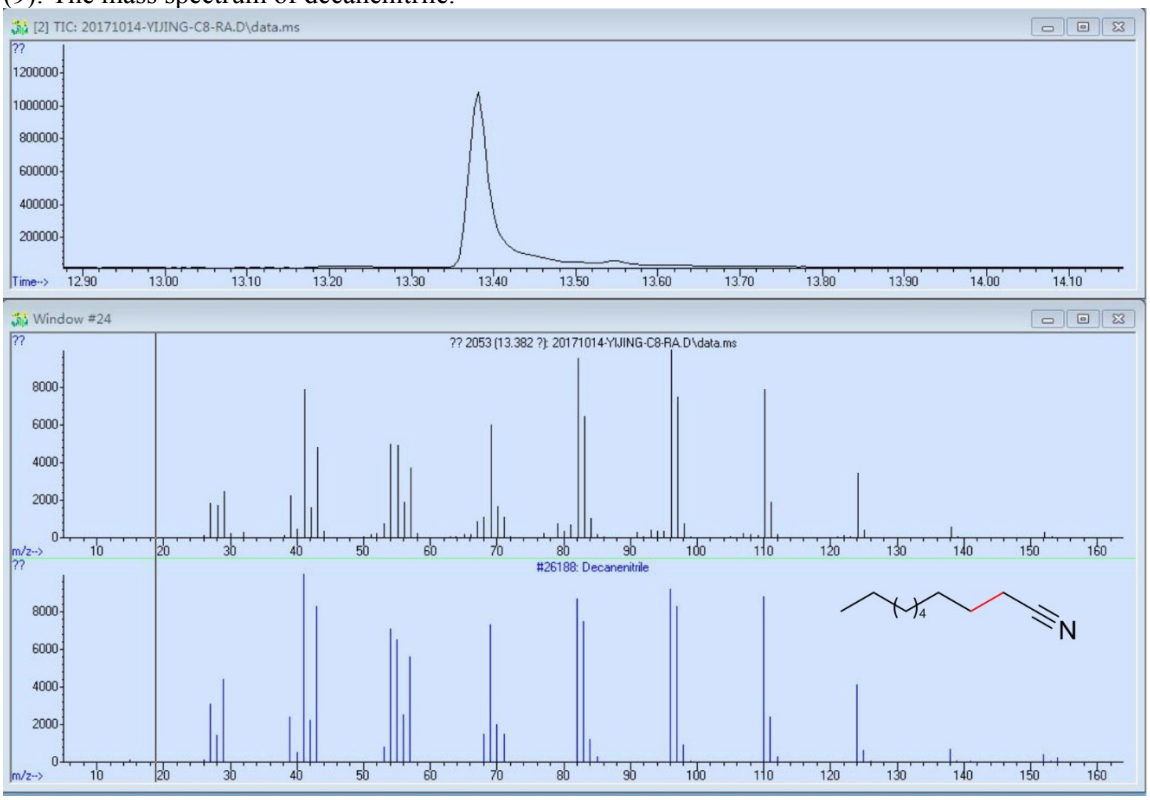

(10): The mass spectrum of nonanenitrile.

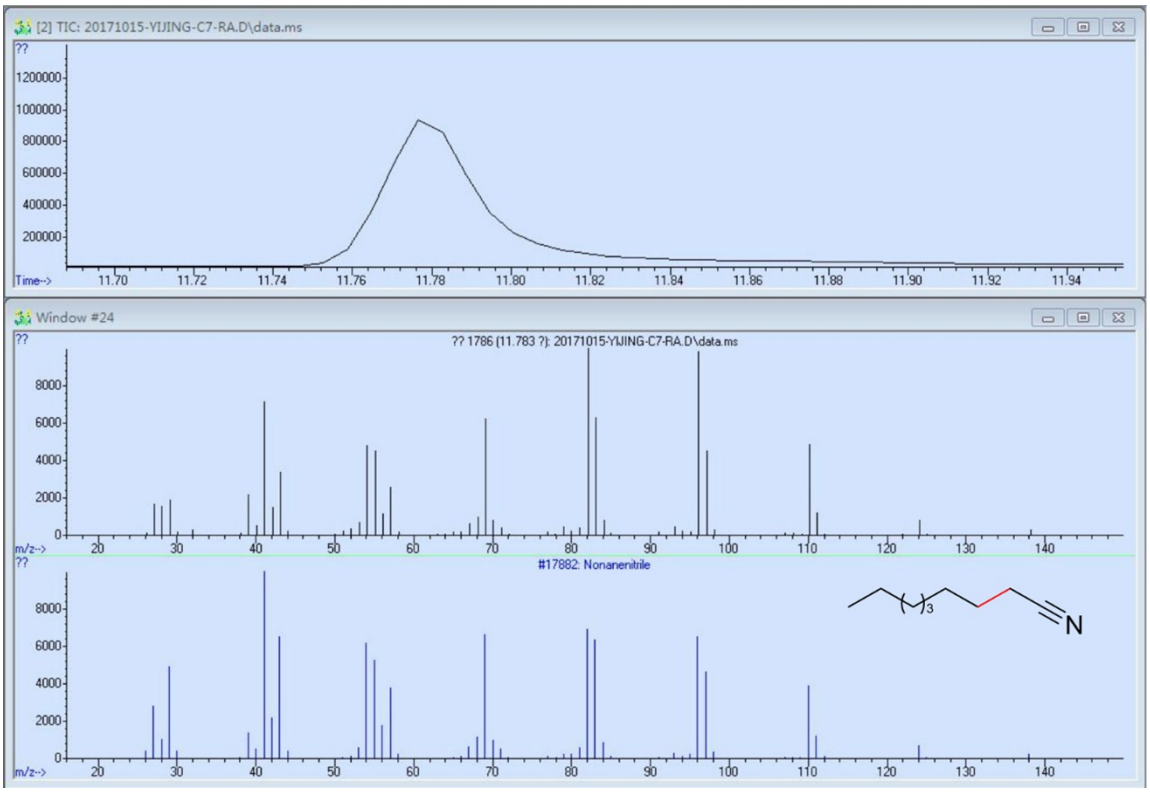

(11): The mass spectrum of dodecanoic acid.

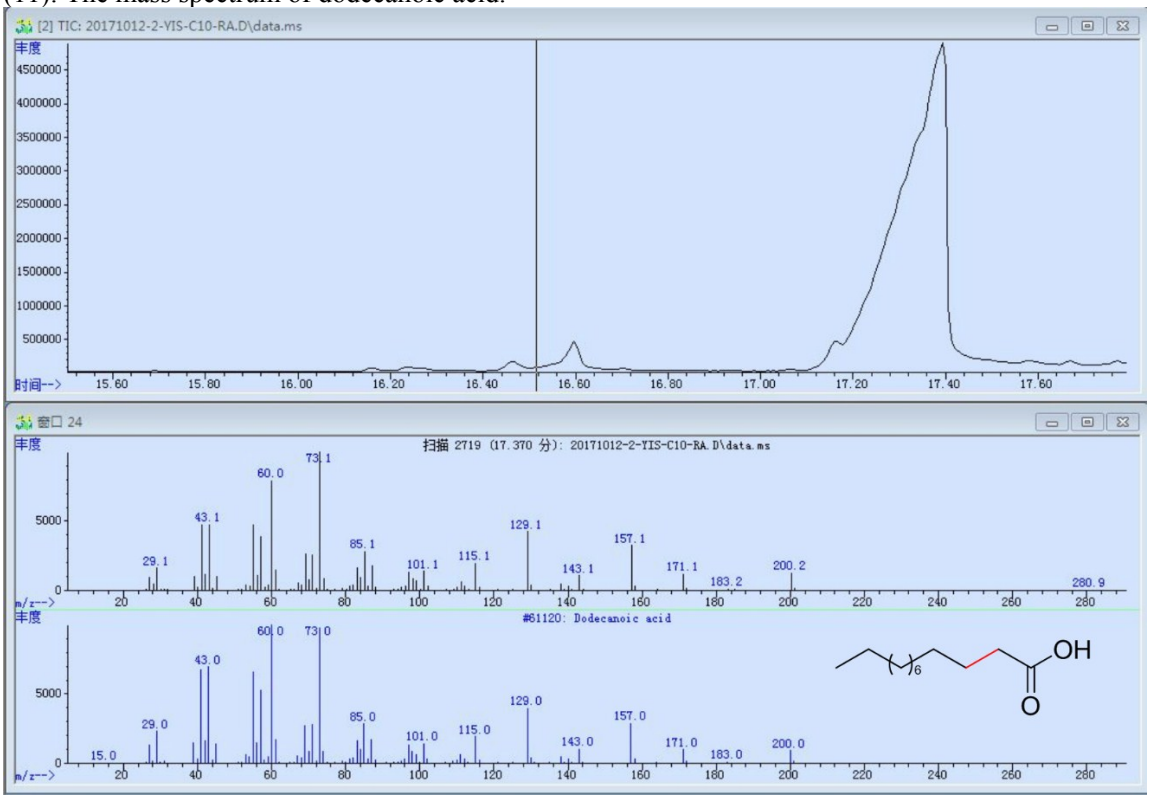

(12): The mass spectrum of undecanoic acid.

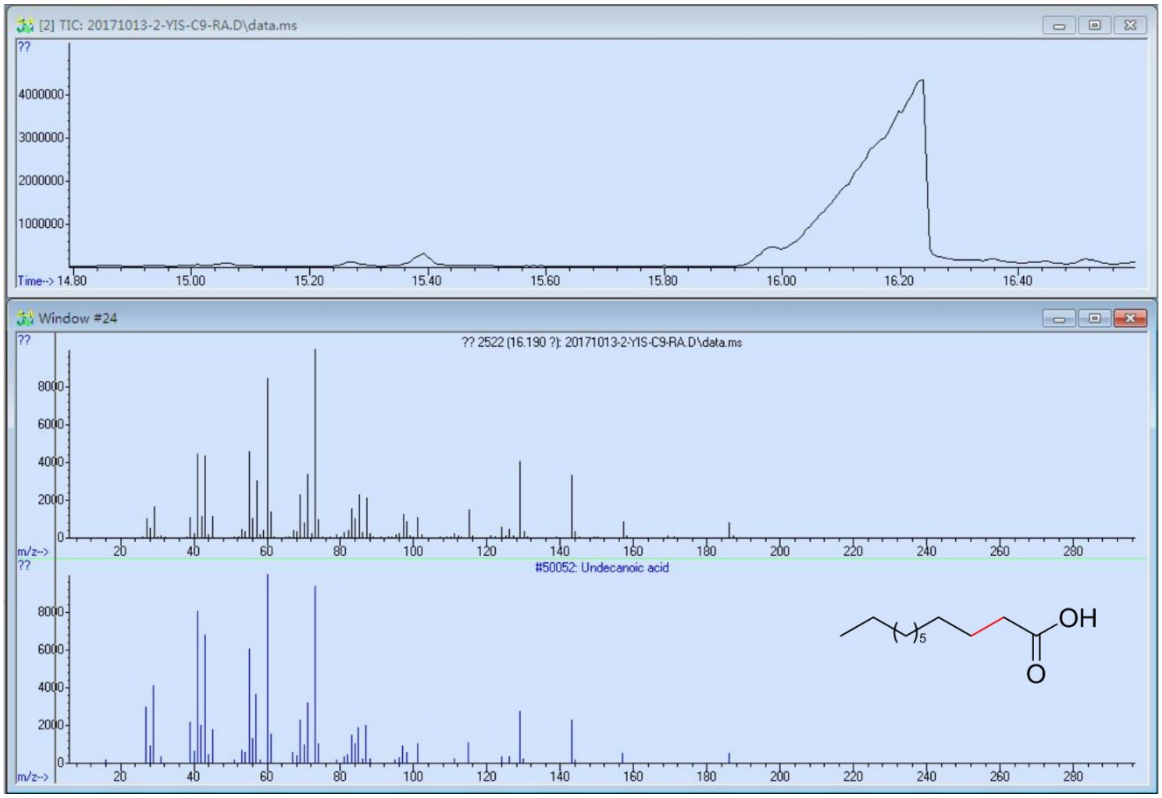

(13): The mass spectrum of decanoic acid.

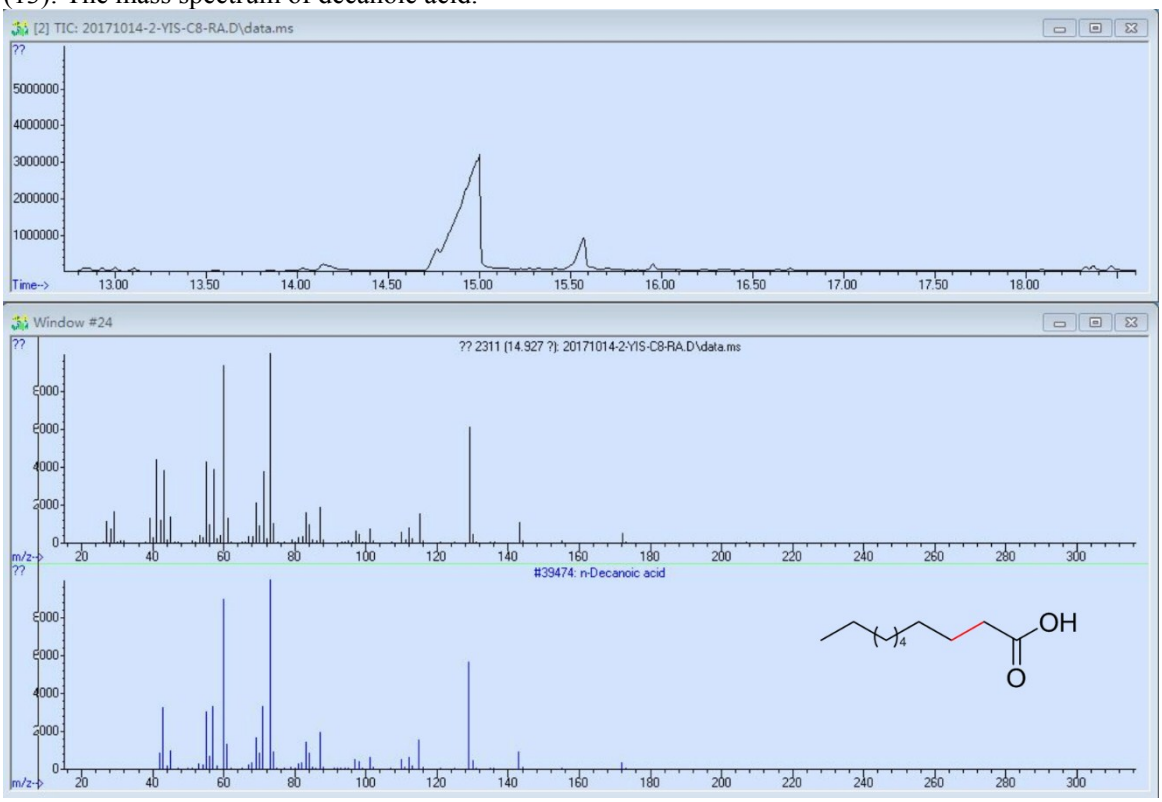

(14): The mass spectrum of nonanoic acid.

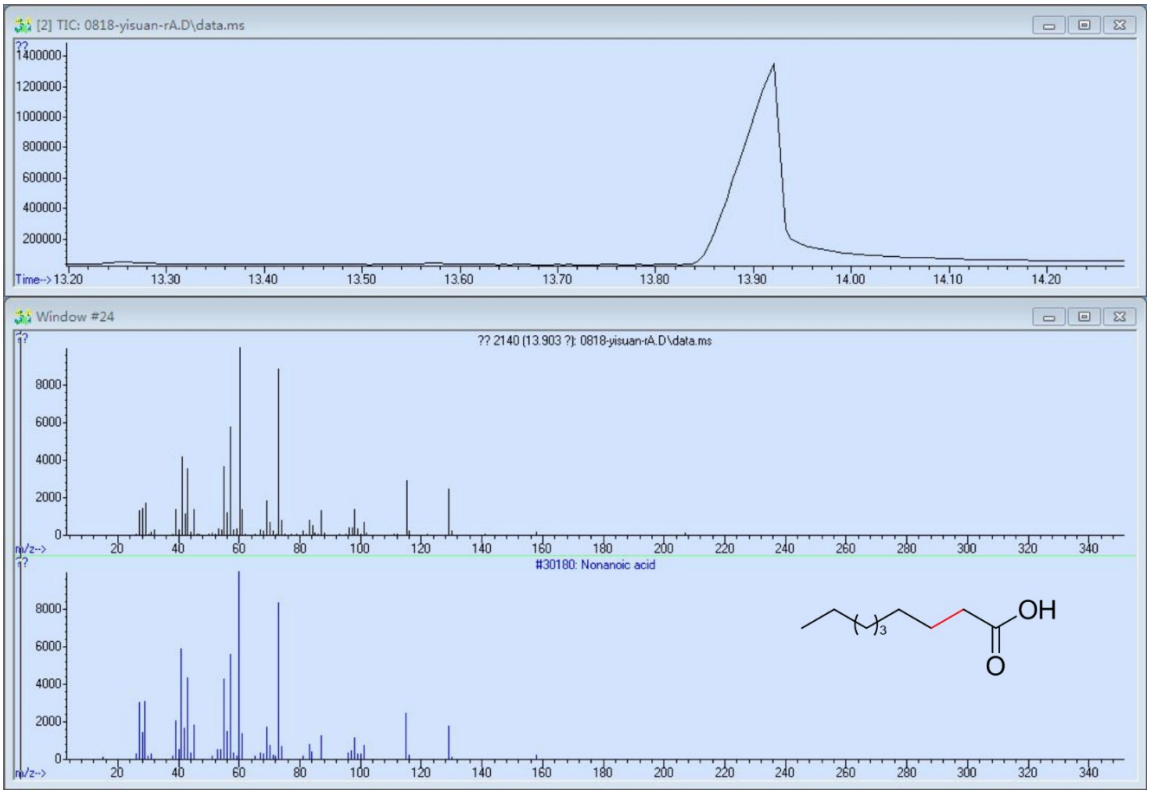

(15): The mass spectrum of dodecan-2-one.

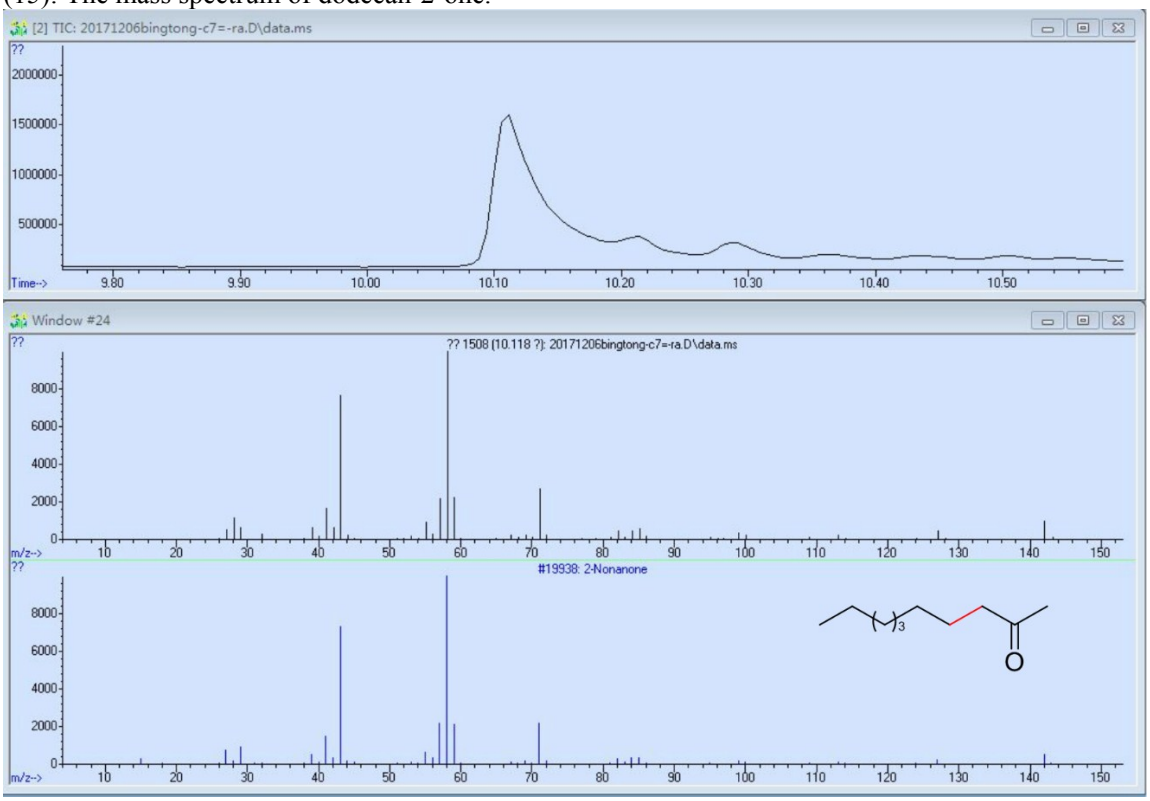

(16): The mass spectrum of ethyl undecanoate

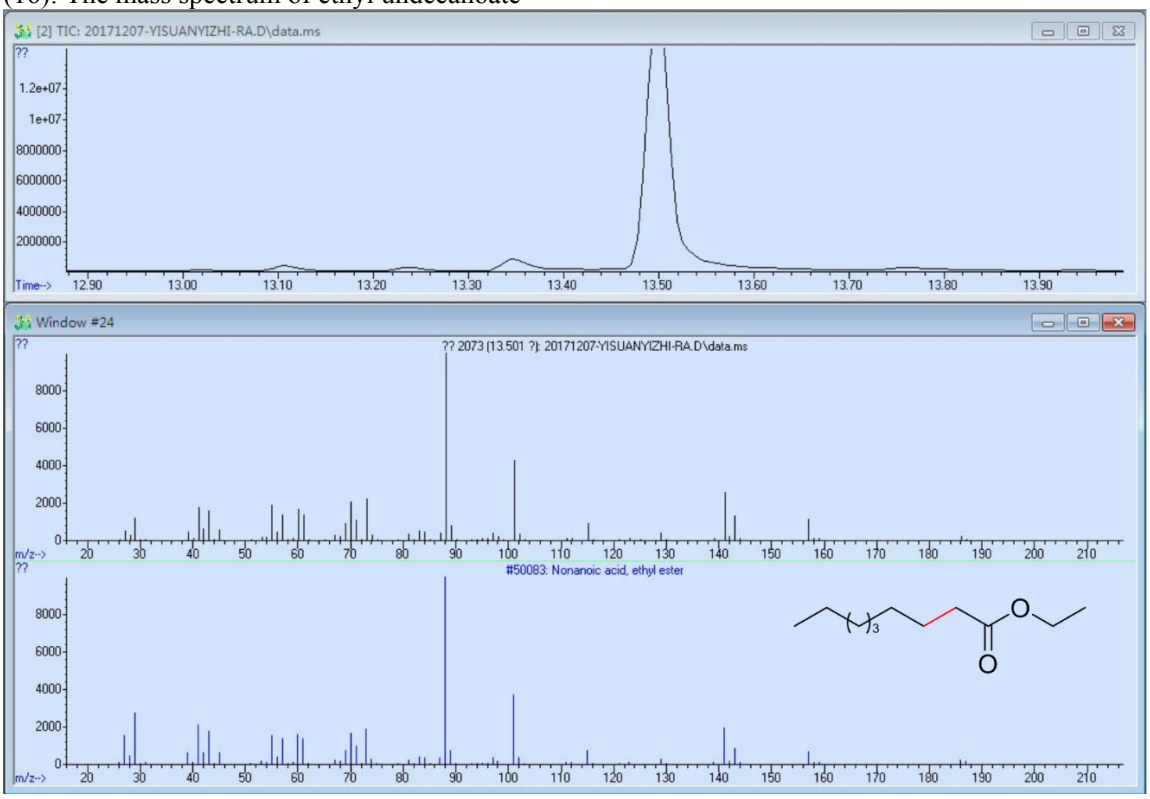

(17): The mass spectrum of deacon-2-ol

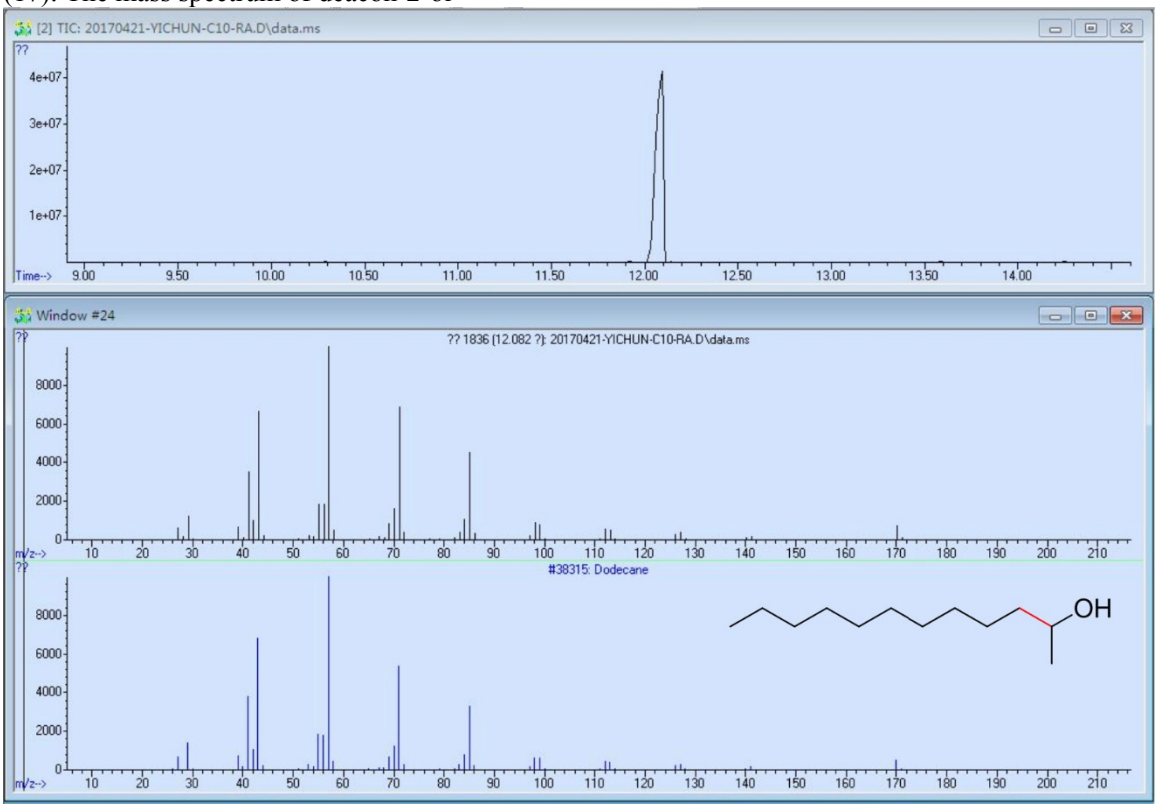

(18): The mass spectrum of tridecan-3-ol

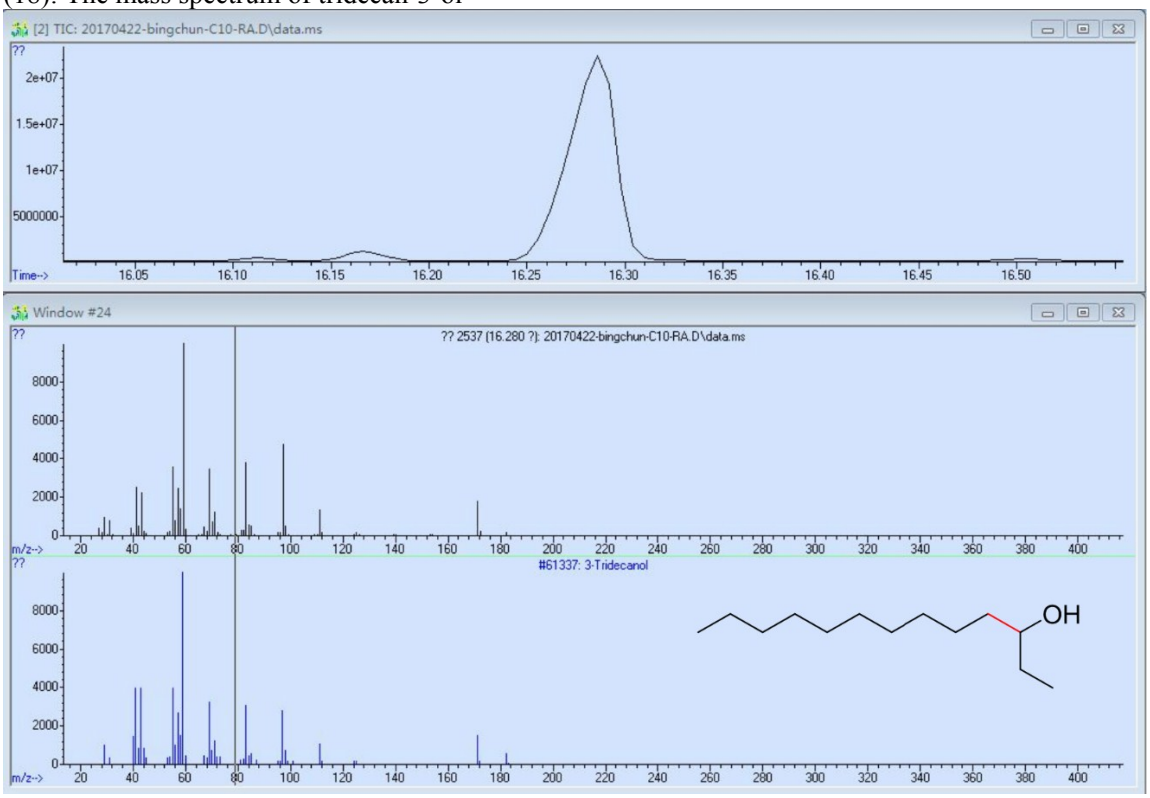

(19): The mass spectrum of 2-methyldodecan-2-ol.

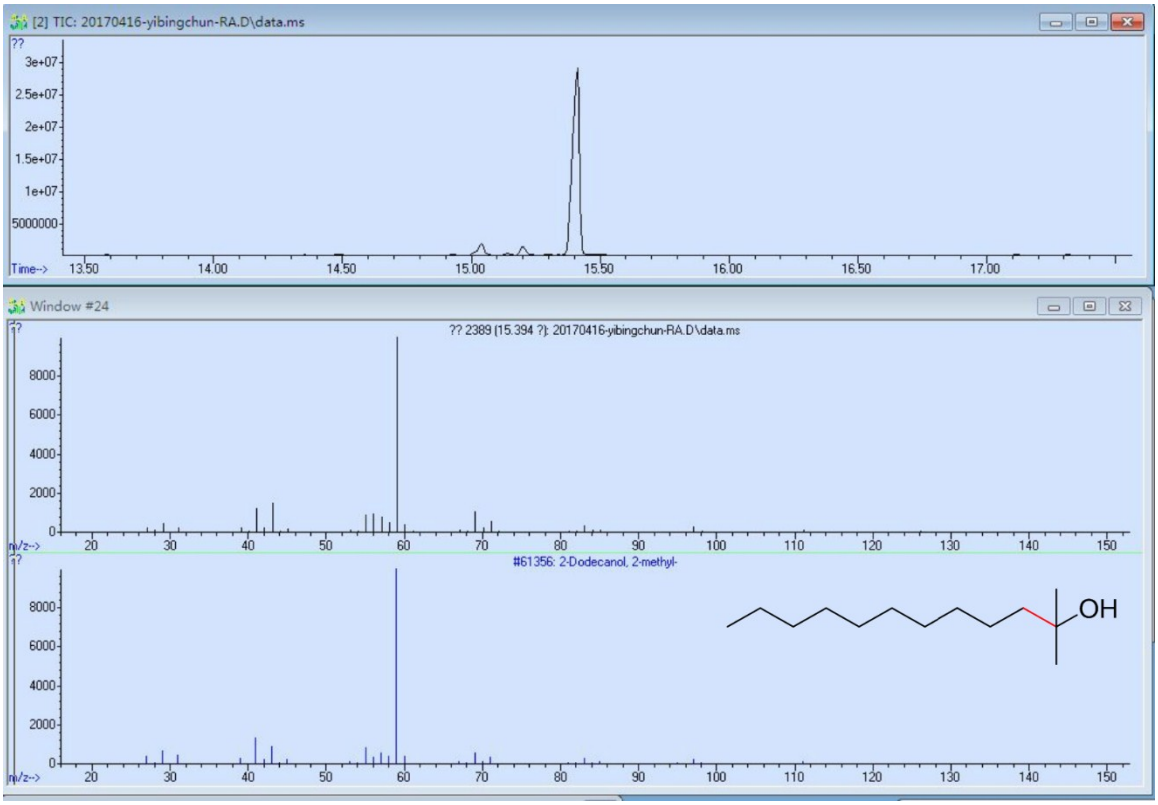

Reference

1 M. J. Frisch, G. W. Trucks, H. B. Schlegel, G. E. Scuseria, M. A. Robb, J. R. Cheeseman, G. Scalmani, V. Barone, B. Mennucci and G. A. Petersson, Gaussian 09, Revision C.01, Gaussian, Inc., Wallingford, CT (2009).

2 A. D. Becke, *J. Chem. Phys.* **1993**, *98*, 5648-5652.

3 N. Godbout, D. R. Salahub, J. Andzelm, E. Wimmer, *Can. J. Chem.* **1992**, *70*, 560-571.

4 AMPAC, Version 9.2.1, Semichem, Inc., 12456 W 62nd Terrace – Suite D, Shawnee, KS 66216 (2008).